Journal of Engineering Mechanics, ASCE, Vol.133, No.10, pp.1101-1114, 2007. 10.

Simple Model of Frequency-Dependent Impedance Functions in Soil-Structure Interaction Using Frequency-Independent Elements

Masato Saitoh

CE Database Keywords: Soil-structure interaction, Elastic foundations, Soil-pile interaction, Dynamic analysis, Embedded foundations, Impedance

ABSTRACT: This study presents a methodology to make a simple equivalent model of frequency-dependent impedance functions of soil-structure interactions using a frequency-independent spring and dashpot, together with a proposed element called "*gyro-mass*". The gyro-mass is frequency-independent and is defined as a unit system that generates a reaction force due to the relative acceleration of the nodes between which the gyro-mass is placed. It is found that a model consisting of a spring, dashpot and gyro-mass may generate various types of frequency-dependent impedance characteristics. This study proposes two types of simple models that express typical frequency-independent impedance functions of soil-structure interactions by using the gyro-mass. The advantage of these models is that the frequency-dependent characteristics can easily be expressed by a small number of elements and degrees of freedom. Moreover, they can be applied directly to conventional time-history analyses, even beyond the elastic region of the structural members. An example in which a simple model is applied to the time-history analysis of a soil-pile-superstructure system with an inelastic structural member when subjected to an earthquake wave is illustrated.

Masato Saitoh, Associate Professor, Department of Civil and Environmental Engineering, Saitama University, 255 Simo-Okubo, Sakura-Ku, Saitama 338-8570, Saitama, Japan
TEL&FAX +81-48-858-3560, e-Mail saity@mail.saitama-u.ac.jp

Journal of Engineering Mechanics, ASCE, Vol.133, No.10, pp.1101-1114, 2007. 10.

INTRODUCTION

Soil-structure interaction (SSI) problems have been studied for about half a century. At present, the characteristics of impedance functions for various soil-structure systems can be estimated with a certain precision by various sophisticated techniques. In general, impedance functions show frequency-dependent characteristics, such as when the soil deposit has layered strata, or the shape and structure of the foundations are complicated, for example, pile groups etc. Therefore, although impedance functions are inappropriate for time-history analysis because of their frequency dependence, they can easily be applied in the frequency domain. However, analyses in the frequency domain are fundamentally restrained within the elastic region of material properties under linear boundary conditions. In contrast, many recent studies of structural dynamics have focused on the inelastic behavior of structural systems because the methodology of performance-based seismic design, which has been applied to seismic codes and guidelines in many countries, allows modeling of the inelastic behavior of structural systems. At present, a number of constitutive models of materials and structural members have been proposed, allowing the inelastic behavior of structural systems during earthquakes to be estimated appropriately. In general, the constitutive models are applied to step-by-step numerical procedures in the time domain because the inelastic behavior of materials and structural members strongly depends on the stress path being integrated stepwise.

In general, impedance functions in SSI show the following typical frequency-dependent characteristics: (a) cut-off frequency below which the damping is negligible and above which the damping increases rapidly (e.g. Novak and Nogami (1977), Nogami and Novak (1977), Kausel and Roesset (1975), Elsabee and Morray (1977), Takemiya and Yamada (1981)); (b) slight oscillation shown in soil reaction and surface rigid foundations or embedded rigid foundations (e.g. Baranov (1967), Beredugo and Novak (1972), Novak (1974), Novak *et al*. (1978), Veletsos and Dotson (1988), Gazetas (1991)); and (c) multiple oscillations typically exhibited in pile groups (e.g. Kaynia and Kausel (1982), Dobry and Gazetas (1988), Makris and Gazetas (1993), Mylonakis and Gazetas (1998)). A variety of methods and techniques by which the frequency-dependent impedance functions can be considered in a time-history analysis have been proposed. From a practical point of view, the most powerful and acceptable tool, not only in the SSI field but also in other engineering fields, is a simple model approximately representing the impedance functions by using the frequency-independent elements of spring, dashpot, and mass [e.g. Meek and Veletsos (1974), Wolf and Somaini (1986), Nogami and Konagai (1986, 1988), Wolf (1994), Wolf and Song (2002)]. The reason for this is that the frequency-independent elements can be applied directly to conventional structural analysis. In recent years, various types of simple models

consisting of these elements (generally called spring-dashpot-mass models) have been proposed for soil reaction, shallow foundations, embedded foundations, etc. Although increasing the number of elements and degrees of freedom results in more accurate fitting to the ideal impedance functions, in practical applications, simple models having a small number of elements and degrees of freedom are used. In general, however, such simple models show a moderate variation with frequency, and thus do not express the frequency-dependent impedance functions with sufficient accuracy.

Moreover, as discussed later, spring-dashpot-mass models are generally not independent systems, so that careful handling is required in the case of seismic excitation when applying them to structural models. Therefore, a simple model that is independent and that can appropriately represent such impedance functions is desired in order to reflect the frequency-dependent characteristics of impedance functions in time-history analysis.

The objectives of the present study are: (1) To introduce a frequency-independent element as an important tool to generate various types of impedance functions; (2) to propose two types of simple models approximately comparable to impedance functions with cut-off frequencies and impedance functions with frequency-dependent oscillations, respectively; (3) to provide the formulae for the impedance functions of the proposed model based on not only dimensionless frequency expressions but also matrix expressions that can directly be incorporated into the conventional structural models; (4) to show examples in which typical impedance functions are simulated by the proposed model, not only in the frequency domain but also in the time domain; and (5) to show an example in which the proposed model is applied to the time-history analysis of a soil-pile-superstructure system including an inelastic structural member when subjected to an earthquake wave. The purpose of this paper is not to provide specific coefficients of the elements by which approximate impedance functions can be easily estimated for individual foundations, but to present a methodology by which a simple model can be made for arbitrary impedance functions.

INTRODUCTION OF PROPOSED FREQUENCY-INDEPENDENT ELEMENT

A representative simple spring-dashpot-mass model used in structural analysis is shown in Fig. 1 (a). To the author's knowledge, this system was first applied by Penzien *et al.* (1964) as a frequency-dependent soil reaction. The equilibrium equation of this system is formulated as

$$F = m\ddot{u} + c\dot{u} + ku \tag{1}$$

where m is the mass; c and k are the damping coefficient and spring coefficient, respectively; F is the external force; and u is the relative displacement of the system.

When a harmonic excitation is assumed, Eq. 1 can be written as

$$F = K^* u \tag{2}$$

where $K^* = \left(k - m\omega^2\right) + ic\omega$, K^* being the impedance function of this system, and ω being the circular frequency. According to Eq. 2, the real part of the impedance function, which represents the stiffness of this system, shows a frequency-dependent characteristic: it decreases gradually as the excitation frequency increases due to the mass effect ($-m\omega^2$). On the other hand, the imaginary part representing the damping effect of the system linearly increases. The above model can be directly used as the impedance function of a soil-foundation system for problems where the structure is excited by loads due to machine vibrations etc. In the case of seismic excitation, however, this has a serious drawback, described below.

Assume that a dynamic displacement u_g is given to the node at the right hand side, as shown in Fig. 1 (b). The node at the left hand side is assumed to be free. The dynamic displacement u_g is analogous to the free-ground response, or the effective foundation input motion in the case of seismic excitation. The relative displacement u appears to be due to the inertial force $m\ddot{u}_g$. In contrast, the actual impedance function generates no relative displacement because it is not actually an oscillator. Practically, therefore, a virtual force is given to the mass for offsetting the inertial force $m\ddot{u}_g$, as shown in Fig. 1 (c). This technique was initially applied to the analysis of soil-pile-structure systems in Penzien *et al.* (1964). This treatment implies that the spring-dashpot-mass system is, in a sense, not an independent system. In addition, there might be a fatal discrepancy between the physical description of the simple model and the actual treatment mentioned above. This discrepancy may induce structural engineers to misunderstand the actual structural systems. From a practical point of view, therefore, careful handling is required when applying such oscillators to structural models.

The simple model should have various frequency dependencies and, in addition, should (a) exhibit independence as a unit impedance system, and (b) describe the system in an identical manner to the actual treatment in the analysis. These characteristics are desired by structural engineers when the frequency-dependent characteristics of impedance functions are considered in

structural analysis.

These desired characteristics can be achieved, to a certain extent, if a so-called "*gyro-mass*" element is introduced in the simple model. The gyro-mass is a frequency-independent element that has the same dimension as mass. It is defined as an independent unit system that generates a reaction force due to the relative acceleration of the nodes between which the gyro-mass is placed, as shown in Fig. 2 (a). The gyro-mass shown in Fig. 2 (a) can be approximated by the simple mechanical analogy shown in Fig. 2 (b). The mechanical analogy consists of a rotational disk and a rod attached to the disk with strong friction, gears for instance. It is assumed that the mass of the rod is negligible. The disk rotates with rotational acceleration $\ddot{\theta}$ as an external force F is given to the rod. The relative acceleration of the rod $\ddot{u}$ with respect to the fixed node at the right hand side is geometrically related to the rotational acceleration $\ddot{\theta}$. Consequently, the following relation between the external force F and the relative acceleration $\ddot{u}$ can be obtained:

$$F = \overline{m}\ddot{u} \tag{3}$$

where

$$\overline{m} \propto \frac{J}{r^2}. \tag{4}$$

Here, r is the distance from the center of the disk to the point where the rod is attached; J is the moment of inertia of the disk; and $\overline{m}$ is the equivalent mass generated by the rotation of the disk. Thus, the reaction force at the left hand side of the rod is identical to the product of the equivalent mass $\overline{m}$ and the relative acceleration $\ddot{u}$. Accordingly, the equivalent mass $\overline{m}$ is termed "gyro-mass" in order to be distinguished from ordinary mass. The above analogy is only an example for explaining the physical feasibility of the gyro-mass element. It is noted that the gyro-mass is not always defined by Eq. 4, but may be defined arbitrarily. In general, the originality of the gyro-mass element proposed in this study lies in its perfect independence: it can take arbitrary values, and it can be freely arranged either in parallel or in series with the other elements in a simple model. The fundamentals of the gyro-mass are explained below.

When an external force F is given to the node at the left hand side of an arbitrary gyro-mass $\overline{m}$ and the other node is fixed, as shown in Fig. 2 (a), the equilibrium equation can be expressed by Eq. 3. When a harmonic excitation is assumed, Eq. 3 can also be expressed by the following formula:

$$F = K^* u \tag{5}$$

where the impedance function $K^* = -\overline{m}\omega^2$. That is, it is found that the impedance function of a gyro-mass becomes a negative value that is proportional to the second power of the excitation frequency.

Consider the model shown in Fig. 3 (a) in which a gyro-mass is used. The equilibrium equation of this model can be expressed as

$$F = \overline{m}\ddot{u} + c\dot{u} + ku . \tag{6}$$

When a harmonic excitation is assumed, Eq. 6 can be rewritten as follows:

$$F = K^* u \tag{7}$$

where the impedance function $K^* = \left(k - \overline{m}\omega^2\right) + ic\omega$. That is, it is found that the impedance function of this model is identical to that of the aforementioned simple spring-dashpot-mass system (Eqs. 1 and 2) if the gyro-mass $\overline{m}$ and the mass m have the same value. Moreover, it is noted that the simple model including a gyro-mass becomes an independent system that satisfies the above-mentioned requirement (a) since no ordinary mass is used. In addition, the description of the model shown in Fig. 3 (a) is compatible with the equilibrium equation derived directly from it. Accordingly, the actual treatment of the model in the structural analysis becomes identical to the configuration in Fig. 3 (a) and Eq. 7. Thus, it is conceivable that the model also satisfies the requirement (b).

In matrix representation, which can be directly applied to conventional structural models, the relation between the external forces (f_1 and f_2) and the absolute displacements (u_1 and u_2) at both nodes of the gyro-mass shown in Fig. 2 (c) can be written as follows:

$$\begin{Bmatrix} f_1 \\ f_2 \end{Bmatrix} = \begin{bmatrix} \overline{m} & -\overline{m} \\ -\overline{m} & \overline{m} \end{bmatrix} \begin{Bmatrix} \ddot{u}_1 \\ \ddot{u}_2 \end{Bmatrix}. \tag{8}$$

It is apparent that the relation of a spring comparable to Eq. 8 can be expressed by the following formula:

$$\begin{Bmatrix} f_1 \\ f_2 \end{Bmatrix} = \begin{bmatrix} k & -k \\ -k & k \end{bmatrix} \begin{Bmatrix} u_1 \\ u_2 \end{Bmatrix} \tag{9}$$

Therefore, the matrix of the gyro-mass can be easily incorporated into structural models, in addition to a spring and a dashpot. Herein, it is presumed that the mechanical analogy of a gyro-mass having free nodes at both sides is difficult to realize perfectly due to the appearance of the inertial force of the disk itself in the lateral direction. In order to enhance the feasibility, the gyro-mass should have a much larger value than the mass of the disk itself. This should be easily accomplished by means of the following conventional techniques used in mechanical engineering: (1) increasing the radius of gyration of the disk by concentrating the mass at the edge of the disk; and (2) increasing the rotational acceleration of the disk by combinations of disk gears. These techniques make the ordinary mass of the disk negligible when compared with the gyro-mass in the system. This issue can be thought of as being analogous to the intrinsic mass of the spring and dashpot in actual mechanical systems.

The simple model shown in Fig. 3 (b) is also expressed by the following formula:

$$\begin{Bmatrix} f_1 \\ f_2 \end{Bmatrix} = \begin{bmatrix} \overline{m} & -\overline{m} \\ -\overline{m} & \overline{m} \end{bmatrix} \begin{Bmatrix} \ddot{u}_1 \\ \ddot{u}_2 \end{Bmatrix} + \begin{bmatrix} c & -c \\ -c & c \end{bmatrix} \begin{Bmatrix} \dot{u}_1 \\ \dot{u}_2 \end{Bmatrix} + \begin{bmatrix} k & -k \\ -k & k \end{bmatrix} \begin{Bmatrix} u_1 \\ u_2 \end{Bmatrix}. \tag{10}$$

This model is very useful, as described later. Therefore, it is defined as a "*base system*" in this study.

PROPOSED SIMPLE MODELS

In this study, typical impedance functions observed in SSI problems are tried to be simulated by using two types of simple models consisting of spring, dashpot and gyro-mass. Hereinafter, a simple model that expresses the cut-off frequency is defined as Type I, while the other model that expresses the frequency-dependent oscillations of impedance functions is defined as Type II.

SIMPLE MODEL: TYPE I

The cut-off frequencies appear in impedance functions of shallow foundations, embedded foundations, and pile foundations, mainly attributable to the effects of layered strata. A simple model is shown in Fig. 4 (a). The model consists of two unit systems: one is the base system mentioned above; and the other is a series system composed of a gyro-mass $\overline{m}$ and a unit having a

spring k and a dashpot c arranged in parallel (this series system is defined as a "*core system*" of the Type I model). The two systems are arranged in parallel in this model. First, the fundamental characteristic of the base system is described below, and the characteristic of the core system is described later.

Base System

The spring, dashpot, and gyro-mass of the base system are defined as K, C and $\overline{M}$, respectively. Referring to the expressions of Wolf and Somaini (1986), the dimensionless frequency a_0 and the dimensionless coefficients of the damper γ_0 and gyro-mass μ_0 are introduced as

$$a_0 = \frac{\omega a}{c_s} \tag{11a}$$

$$C = \frac{a}{c_s} K\gamma_0 \tag{11b}$$

$$\overline{M} = \frac{a^2}{c_s^2} K\mu_0 \tag{11c}$$

where a represents a characteristic length of the foundation (e.g. the radius of a disc) and c_s denotes the shear wave velocity. The equilibrium equation of the base system is analogous to Eq. 7. Substituting Eq. 11 into Eq. 7 yields

$$F(a_0) = K\left(1 - \mu_0 a_0^2 + i\, a_0 \gamma_0\right) u(a_0). \tag{12}$$

Fig. 5 shows the variation of the impedance functions given by Eq. 12. Fig. 5 shows that the stiffness (the real part of the impedance function) decreases gradually as the excitation frequency increases. This decrease in the stiffness becomes significant as the coefficient of the gyro-mass μ_0 increases. On the one hand, the damping (the imaginary part of the impedance function) increases linearly as the frequency increases. The coefficient of the damper γ_0 is associated with the gradient of the damping.

Core System of Type I model

When an external force F is given to the node at the left hand side of the core system and the other node is fixed, as shown in Fig. 4 (b), the equilibrium equation of the core system can be expressed as follows:

$$F = \overline{m}\Delta\ddot{u}_I \tag{13a}$$

$$F = k\Delta u_E + c\Delta\dot{u}_E \tag{13b}$$

where Δu_I is the relative displacement of the gyro-mass and Δu_E is the relative displacement of the spring and the dashpot. The total relative displacement u of this system becomes the sum of the relative displacements Δu_I and Δu_E. When a harmonic external force is assumed, the following relation can be derived from Eqs. 13a and 13b:

$$F(\omega) = k\left[\frac{\frac{\overline{m}\omega^2}{k}\left(\frac{\overline{m}\omega^2}{k} - \frac{c^2\omega^2}{k^2} - 1\right)}{\left(1 - \frac{\overline{m}\omega^2}{k}\right)^2 + \frac{c^2\omega^2}{k^2}} + i\omega\frac{\frac{\overline{m}\omega^2}{k}\frac{\overline{m}c\omega^2}{k^2}}{\left(1 - \frac{\overline{m}\omega^2}{k}\right)^2 + \frac{c^2\omega^2}{k^2}}\right]u(\omega). \tag{14}$$

The dimensionless coefficients of the damper γ_1 and the gyro-mass μ_1 are introduced as:

$$c = \frac{a}{c_s}k\gamma_1 \tag{15a}$$

$$\overline{m} = \frac{a^2}{c_s^2}k\mu_1. \tag{15b}$$

By using Eq. 15, Eq. 14 can be transformed to

$$F(a_0) = k\left[\frac{\mu_1 a_0^2\left(\mu_1 a_0^2 - \gamma_1^2 a_0^2 - 1\right)}{\left(1 - \mu_1 a_0^2\right)^2 + \gamma_1^2 a_0^2} + i\,a_0\frac{\gamma_1\mu_1^2 a_0^4}{\left(1 - \mu_1 a_0^2\right)^2 + \gamma_1^2 a_0^2}\right]u(a_0) \tag{16}$$

Fig. 6 shows the a_0 variation of the impedance function of the system. Fig. 6 (b) indicates that the damping increases rapidly around the dimensionless frequency $a_0 = 1$. This characteristic is quite

analogous to typical impedance functions having a cut-off frequency. On the other hand, the stiffness becomes zero in the lower frequency region, and it tends to show a local minimum around the cut-off frequency, as shown in Fig. 6 (a). In addition, it is found that the impedance function changes substantially as the coefficient of the damper γ_1 decreases. Therefore, the coefficient γ_1 is associated with the sensitivity of the impedance function to the cut-off frequency. The cut-off frequency is considered to be almost identical to the singular point of Eq. 16 when the coefficient γ_1 takes a very small value. Thus, the cut-off frequency is defined as

$$a_c = \frac{1}{\sqrt{\mu_1}}. \tag{17}$$

Therefore, it is noted that the coefficient of the gyro-mass μ_1 is associated with the cut-off frequency of the core system.

The reason why the cut-off frequency appears in the core system consisting of only three elements can be explained as follows. In the lower frequency region, the characteristic of the impedance function of the core system is highly influenced by the impedance function of the gyro-mass since the impedance function of the gyro-mass becomes smaller than that of the unit composed of the spring k and the dashpot c; that is, the displacement of the core system is mainly generated by the gyro-mass in this frequency region. In contrast, in the higher frequency region, the characteristic of the impedance function of the core system is highly influenced by the impedance function of the unit composed of the spring k and the dashpot c since the impedance function of this unit becomes smaller than that of the gyro-mass; that is, the displacement of the core system is mainly generated by this unit in the higher frequency region. Therefore, the cut-off frequency is almost identical to the frequency around which the impedance function of the core system changes from that of the gyro-mass to that of the spring/dashpot unit.

Total System of Type I model

In the Type I model, the core system and the base system are arranged in parallel. Hence, the impedance function of this model is consistent with the sum of both impedance functions. Referring to Eqs. 12 and 16, the equilibrium equation of Type I is expressed by the following formula:

$$F(a_0) = K\left\{1 + \frac{\beta_1 \mu_1 a_0^2 \left(\mu_1 a_0^2 - \gamma_1^2 a_0^2 - 1\right)}{\left(1 - \mu_1 a_0^2\right)^2 + \gamma_1^2 a_0^2} - \mu_0 a_0^2 + i\, a_0 \left[\frac{\beta_1 \gamma_1 \mu_1^2 a_0^4}{\left(1 - \mu_1 a_0^2\right)^2 + \gamma_1^2 a_0^2} + \gamma_0\right]\right\} u(a_0) \qquad (18)$$

where $\beta_1 = k/K$.

In this model, the coefficient K is compatible with the static stiffness ($a_0 = 0$). β_1 denotes the weight function of the core system with respect to the base system. In principle, the other coefficients used in this model play the same role as shown in the individual systems described above since the base system and the core system are merely arranged in parallel. It is noted that the important feature of this model is that the characteristics of the individual parameters are identified so that the fitting of impedance functions by using this model is fairly easy. At present, manual fitting is the main technique used for simulating arbitrary impedance functions in this study. In future, a more advanced numerical fitting technique may be developed.

Fig. 7 shows a comparison of the impedance functions of a pile in vertical vibration evaluated using Eq. 18 with published results of a rigorous solution (Novak and Nogami (1977)). The properties assumed in the rigorous solution were as follows: slenderness ratio $H/r_0 = 40$; mass ratio $\overline{\rho} = 0.6$; damping ratio of soil $D = 0.02$; Poisson's ratio $\nu = 0$; and dimensionless parameter related to the stiffness ratio $Y = 10$. This impedance function is a typical function having a cut-off frequency. Fig. 7 indicates that the behavior around the cut-off frequency ($a_0 \cong 0.05$) exhibited in the rigorous solution is very similar to that of the simple model proposed here. Apparently, the installation of the gyro-mass in the core system is responsible for the appearance of the local minimum of the stiffness and the rapid increase of the damping around the cut-off frequency.

Fig. 8 (a) also shows the comparison of the impedance functions of a pile in horizontal vibration evaluated using Eq. 18 with published results of the rigorous solution (Novak and Nogami (1977)). The properties assumed in the rigorous solution were the same as the above, except for the dimensionless parameter $Y = 1000$. In the simulation, the dimensionless static stiffness $K^* H^3 / E_p I$ ($a_0 = 0$) is assumed to be 226.0, where E_p and I are the Young's modulus and the geometrical moment of inertia of the pile, respectively.

Since the simple model exhibits only one cut-off frequency, the double cut-off frequencies appearing around the dimensionless frequencies $a_0 = 0.05$ and $a_0 = 0.15$ in the rigorous solution cannot be simulated sufficiently if the higher frequency region is considered to be important. In order to enhance the precision of the simulation, if needed, an additional core system having

different coefficients can be arranged in parallel with the Type I model. Fig. 8 (b), which shows the simulated impedance functions of this revised model, shows that two cut-off frequencies appear in the impedance functions of the model. In addition, the behavior of the impedance functions is also very similar to the rigorous solutions over the entire dimensionless frequency range. Herein, the impedance functions of a generalized Type I model having multiple core systems, shown in Fig. 9, can be expressed by the following formula:

$$F\left(a_0\right)=K\left\{1+\sum_{i=1}^{N}\frac{\beta_i\mu_i a_0^2\left(\mu_i a_0^2-\gamma_i^2 a_0^2-1\right)}{\left(1-\mu_i a_0^2\right)^2+\gamma_i^2 a_0^2}-\mu_0 a_0^2+i\,a_0\left[\sum_{i=1}^{N}\frac{\beta_i\gamma_i\mu_i^2 a_0^4}{\left(1-\mu_i a_0^2\right)^2+\gamma_i^2 a_0^2}+\gamma_0\right]\right\}u\left(a_0\right) \quad (19)$$

where γ_i, μ_i, and β_i are, respectively, the dimensionless coefficients of the damper and the gyro-mass, and the stiffness ratio of the i th core system shown in Fig. 9; and N is the total number of core systems.

SIMPLE MODEL: TYPE II

Hereinafter, typical impedance functions having frequency-dependent oscillations are simulated by a Type II model. The simple model is shown in Fig. 10 (a). The Type II model consists of two unit systems: one is the base system described above; and the other is a series system composed of a spring k and a unit having a gyro-mass $\overline{m}$ and a dashpot c arranged in parallel (this series system is also defined as a core system of the Type II model). The base system and the core system are arranged in parallel.

Core system of Type II model

The core system of the Type II model is identical to a system in which the positions of the spring and the gyro-mass in the core system of the Type I model are exchanged. Referring to the derivation shown in the Type I model, the relation between the external force F and the relative displacement u of the core system of the Type II model shown in Fig.10 (b) can be obtained as follows:

$$F\left(\omega\right)=k\left[\frac{\frac{\omega^2\overline{m}}{k}\left(\frac{\omega^2\overline{m}}{k}-1\right)+\frac{\omega^2c^2}{k^2}}{\left(1-\frac{\omega^2\overline{m}}{k}\right)^2+\frac{\omega^2c^2}{k^2}}+i\omega\frac{\frac{c}{k}}{\left(1-\frac{\omega^2\overline{m}}{k}\right)^2+\frac{\omega^2c^2}{k^2}}\right]u\left(\omega\right) \quad (20)$$

By using the dimensionless frequency and the dimensionless coefficients, Eq. 20 can be transformed to

$$F(a_0) = k\left[\frac{\mu_1 a_0^2(\mu_1 a_0^2 - 1) + \gamma_1^2 a_0^2}{(1-\mu_1 a_0^2)^2 + \gamma_1^2 a_0^2} + i\, a_0 \frac{\gamma_1}{(1-\mu_1 a_0^2)^2 + \gamma_1^2 a_0^2}\right] u(a_0). \quad (21)$$

Fig. 11 shows the a_0 variation of the impedance function of the core system. It is found that a variety of impedance functions of the system can be generated as the coefficient of the damper γ_1 changes. Fig. 11 indicates that the stiffness changes substantially, whereas the damping exhibits a local maximum around the dimensionless frequency $a_0 = 1$ when the dimensionless coefficient γ_1 takes a small value. The reason for this is that the impedance function of this core system has a singular point when the coefficient γ_1 takes a very small value. This characteristic is identical to that of the core system in the Type I model. Therefore, this resonant frequency is the same as the cut-off frequency in the Type I model obtained from Eq. 17.

Total system of Type II model

The equilibrium equation of the Type II model is expressed as the sum of Eqs. 12 and 21, as follows:

$$F(a_0) = K\left\{1 + \frac{\beta_1\left[\mu_1 a_0^2(\mu_1 a_0^2 - 1) + \gamma_1^2 a_0^2\right]}{(1-\mu_1 a_0^2)^2 + \gamma_1^2 a_0^2} - \mu_0 a_0^2 + i\, a_0\left[\frac{\beta_1\gamma_1}{(1-\mu_1 a_0^2)^2 + \gamma_1^2 a_0^2} + \gamma_0\right]\right\} u(a_0) \quad (22)$$

Hereinafter, representative impedance functions having the two types of oscillation mentioned above are simulated by using the Type II model.

Fig. 12 shows a comparison of the impedance functions of soil reaction in horizontal and vertical vibrations simulated by the Type II model with the published results of a rigorous solution (Novak (1974)). The dimensionless coefficients used in this analysis are shown in Table. 1. The impedance functions are normalized by the shear modulus of the soil G_s. It is assumed that these impedance functions are typical functions having a slight oscillation. Fig. 12 shows that the impedance functions simulated by the Type II model are very similar to those of the rigorous solution. Since the Type II model is a three-degree-of-freedom system with a total of six elements,

this model can simulate the impedance function with fewer elements and degrees of freedom than the models proposed previously, and with almost the same precision. Moreover, it is noted that the present model consists of no ordinary mass; therefore, the model can be treated as an independent system.

Fig. 13 shows a comparison of a horizontal impedance function of a 2 × 2 pile group (stiffness ratio of pile to soil $E_p/E_s = 1000$, slenderness ratio $H/d = 15$, Poisson's ratio $\nu = 0.4$, material damping of soil $\beta_s = 0.05$) simulated by the Type II model with the published results of a rigorous solution (Kaynia and Kausel (1982)) for a variety of S/d ratios, where S is the axis-to-axis distance of the piles and d is the diameter of the piles. The dimensionless coefficients used in this analysis are shown in Table 2. Figs. 13 (a) and (b) show the results simulated by using the Type II model with a single core system. The agreement is good below the dimensionless frequency at which the local maxima of the impedance functions appear. In the higher frequency region, however, a discrepancy appears between the simulated impedance functions and the rigorous solution. In order to enhance the precision of the simulation, if needed, an additional core system having different coefficients can be arranged in parallel with the Type II model. For example, Figs. 13 (c) and (d) show the simulated impedance functions of a revised model consisting of double core systems. The results show better agreement between the simulated results and the rigorous solution in the higher frequency region than the model having a single core system. Herein, the impedance functions of the generalized Type II model having multiple core systems shown in Fig. 14 can be expressed by the following formula:

$$F(a_0) = K\left\{1 + \sum_{i=1}^{N} \frac{\beta_i\left[\mu_i a_0^2\left(\mu_i a_0^2 - 1\right) + \gamma_i^2 a_0^2\right]}{\left(1 - \mu_i a_0^2\right)^2 + \gamma_i^2 a_0^2} - \mu_0 a_0^2 + i\, a_0\left[\sum_{i=1}^{N} \frac{\beta_i \gamma_i}{\left(1 - \mu_i a_0^2\right)^2 + \gamma_i^2 a_0^2} + \gamma_0\right]\right\} u(a_0). \tag{23}$$

MATRIX EXPRESSIONS OF SIMPLE MODELS

As mentioned above, the matrix representation of the simple models is very convenient in practice since this representation is directly applicable to conventional structural models. Therefore, the matrix expressions of both simple models are presented below.

The core system of the Type I model shown in Fig. 4 (a) can be formulated as

$$\begin{Bmatrix} f_1 \\ f_2 \\ f_3 \end{Bmatrix} = \begin{bmatrix} \overline{m} & -\overline{m} & 0 \\ -\overline{m} & \overline{m} & 0 \\ 0 & 0 & 0 \end{bmatrix} \begin{Bmatrix} \ddot{u}_1 \\ \ddot{u}_2 \\ \ddot{u}_3 \end{Bmatrix} + \begin{bmatrix} 0 & 0 & 0 \\ 0 & c & -c \\ 0 & -c & c \end{bmatrix} \begin{Bmatrix} \dot{u}_1 \\ \dot{u}_2 \\ \dot{u}_3 \end{Bmatrix} + \begin{bmatrix} 0 & 0 & 0 \\ 0 & k & -k \\ 0 & -k & k \end{bmatrix} \begin{Bmatrix} u_1 \\ u_2 \\ u_3 \end{Bmatrix} \tag{24}$$

where u_1, u_2 and u_3 are the absolute displacements of the nodes; and f_1, f_2 and f_3 are the external forces of the nodes.

Therefore, referring to Eq. 10, the Type I model can be expressed as:

$$\begin{Bmatrix} f_1 \\ f_2 \\ f_3 \end{Bmatrix} = \begin{bmatrix} \overline{M}+\overline{m} & -\overline{m} & -\overline{M} \\ -\overline{m} & \overline{m} & 0 \\ -\overline{M} & 0 & \overline{M} \end{bmatrix} \begin{Bmatrix} \ddot{u}_1 \\ \ddot{u}_2 \\ \ddot{u}_3 \end{Bmatrix} + \begin{bmatrix} C & 0 & -C \\ 0 & c & -c \\ -C & -c & C+c \end{bmatrix} \begin{Bmatrix} \dot{u}_1 \\ \dot{u}_2 \\ \dot{u}_3 \end{Bmatrix} + \begin{bmatrix} K & 0 & -K \\ 0 & k & -k \\ -K & -k & K+k \end{bmatrix} \begin{Bmatrix} u_1 \\ u_2 \\ u_3 \end{Bmatrix}. \tag{25}$$

Moreover, the generalized Type I model shown in Fig. 9 can be formulated as:

$$\begin{Bmatrix} f_1 \\ f_{21} \\ f_{22} \\ \vdots \\ f_{2N} \\ f_3 \end{Bmatrix} = [M_N] \begin{Bmatrix} \ddot{u}_1 \\ \ddot{u}_{21} \\ \ddot{u}_{22} \\ \vdots \\ \ddot{u}_{2N} \\ \ddot{u}_3 \end{Bmatrix} + [C_N] \begin{Bmatrix} \dot{u}_1 \\ \dot{u}_{21} \\ \dot{u}_{22} \\ \vdots \\ \dot{u}_{2N} \\ \dot{u}_3 \end{Bmatrix} + [K_N] \begin{Bmatrix} u_1 \\ u_{21} \\ u_{22} \\ \vdots \\ u_{2N} \\ u_3 \end{Bmatrix} \tag{26a}$$

where,

$$[M_N] = \begin{bmatrix} \overline{M}+\sum_{i=1}^{N}\overline{m}_i & -\overline{m}_1 & -\overline{m}_2 & \cdots & -\overline{m}_N & -\overline{M} \\ -\overline{m}_1 & \overline{m}_1 & 0 & \cdots & 0 & 0 \\ -\overline{m}_2 & 0 & \overline{m}_2 & \cdots & 0 & 0 \\ \vdots & \vdots & \vdots & \ddots & \vdots & \vdots \\ -\overline{m}_N & 0 & 0 & \cdots & \overline{m}_N & 0 \\ -\overline{M} & 0 & 0 & \cdots & 0 & \overline{M} \end{bmatrix} \tag{26b}$$

$$[C_N]=\begin{bmatrix} C & 0 & 0 & \cdots & 0 & -C \\ 0 & c_1 & 0 & \cdots & 0 & -c_1 \\ 0 & 0 & c_2 & \cdots & 0 & -c_2 \\ \vdots & \vdots & \vdots & \ddots & \vdots & \vdots \\ 0 & 0 & 0 & \cdots & c_N & -c_N \\ -C & -c_1 & -c_2 & \cdots & -c_N & C+\sum_{i=1}^{N} c_i \end{bmatrix} \tag{26c}$$

$$[K_N]=\begin{bmatrix} K & 0 & 0 & \cdots & 0 & -K \\ 0 & k_1 & 0 & \cdots & 0 & -k_1 \\ 0 & 0 & k_2 & \cdots & 0 & -k_2 \\ \vdots & \vdots & \vdots & \ddots & \vdots & \vdots \\ 0 & 0 & 0 & \cdots & k_N & -k_N \\ -K & -k_1 & -k_2 & \cdots & -k_N & K+\sum_{i=1}^{N} k_i \end{bmatrix} \tag{26d}$$

where u_{2i} is the absolute displacement of the node in the *i* th core system; and c_i, $\overline{m}_i$, and k_i are, respectively, the coefficients of the damper, the gyro-mass, and the stiffness of the *i* th core system shown in Fig. 9.

Recall that the difference between the Type I and Type II models is that the positions of the spring and the gyro-mass in the core system are merely exchanged. Therefore, the Type II model shown in Fig. 10 (a) can be expressed as follows:

$$\begin{Bmatrix} f_1 \\ f_2 \\ f_3 \end{Bmatrix}=\begin{bmatrix} \overline{M} & 0 & -\overline{M} \\ 0 & \overline{m} & -\overline{m} \\ -\overline{M} & -\overline{m} & \overline{M}+\overline{m} \end{bmatrix}\begin{Bmatrix} \ddot{u}_1 \\ \ddot{u}_2 \\ \ddot{u}_3 \end{Bmatrix}+\begin{bmatrix} C & 0 & -C \\ 0 & c & -c \\ -C & -c & C+c \end{bmatrix}\begin{Bmatrix} \dot{u}_1 \\ \dot{u}_2 \\ \dot{u}_3 \end{Bmatrix}+\begin{bmatrix} K+k & -k & -K \\ -k & k & 0 \\ -K & 0 & K \end{bmatrix}\begin{Bmatrix} u_1 \\ u_2 \\ u_3 \end{Bmatrix}. \tag{27}$$

Moreover, the generalized Type II model shown in Fig. 14 can be expressed by the same equation as Eq. 26 (a), except for the components of $[M_N]$ and $[K_N]$, which are:

$$[M_N]=\begin{bmatrix} \overline{M} & 0 & 0 & \cdots & 0 & -\overline{M} \\ 0 & \overline{m}_1 & 0 & \cdots & 0 & -\overline{m}_1 \\ 0 & 0 & \overline{m}_2 & \cdots & 0 & -\overline{m}_2 \\ \vdots & \vdots & \vdots & \ddots & \vdots & \vdots \\ 0 & 0 & 0 & \cdots & \overline{m}_N & -\overline{m}_N \\ -\overline{M} & -\overline{m}_1 & \overline{m}_2 & \cdots & -\overline{m}_N & \overline{M}+\sum_{i=1}^{N}\overline{m}_i \end{bmatrix} \tag{28a}$$

$$[K_N]=\begin{bmatrix} K+\sum_{i=1}^{N}k_i & -k_1 & -k_2 & \cdots & -k_N & -K \\ -k_1 & k_1 & 0 & \cdots & 0 & 0 \\ -k_2 & 0 & k_2 & \cdots & 0 & 0 \\ \vdots & \vdots & \vdots & \ddots & \vdots & \vdots \\ -k_N & 0 & 0 & \cdots & k_N & 0 \\ -K & 0 & 0 & \cdots & 0 & K \end{bmatrix}. \tag{28b}$$

COMPARISON WITH IMPEDANCE FUNCTIONS IN TIME DOMAIN

A comparison of the impedance functions evaluated in the frequency domain with those evaluated in the time domain is shown below. For this comparison, the generalized Type II model shown in Fig. 14 is used. The properties of the dimensionless coefficients are identical to the model in the case of $S/d=10$ shown in Table. 2. In this analysis, the parameter a/c_s and the static stiffness K are assumed to be 0.02 sec and 240000 kN/m, respectively. Referring to Eqs. 11 and 15, the coefficients of this model can be estimated as follows: $k_1=225600$ kN/m; $k_2=240000$ kN/m; $C=864$ kN-sec/m; $c_1=18048$ kN-sec/m; $c_2=2880$ kN-sec/m; $\overline{M}=124.8$ t; $\overline{m}_1=721.9$ t; and $\overline{m}_2=91.2$ t. As a numerical integration scheme, Newmark's β method is applied ($\beta=1/6$). In the analysis, a harmonic external force is given to the node at one side of the model shown in Fig.14, and the node at the other side of the model is fixed. Fig. 15 shows a comparison of the impedance function in the frequency domain evaluated directly from Eq. 23 with the solutions based on Eqs. 26 and 28 in the time domain. Good agreement between the frequency-domain and time-domain impedance functions can be seen in the figure. It is noted, therefore, that the frequency-dependent impedance functions can be precisely expressed by using the simple models in the time domain.

APPLICATION TO NONLINEAR TIME-HISTORY ANALYSIS

This study shows an example of time-history analysis of a structural system subjected to an earthquake wave. As shown in Fig. 16, the structural system consists of a superstructure, which is represented by an inelastic one-degree-of-freedom system, and an elastic soil-pile system represented by a footing mass and the Type II model proposed above. It is assumed that the properties of the soil-pile system are identical to the model used in the above comparison. For simplicity, as an example, the footing is assumed to be free only in the lateral direction, whereas the movements of the footing are completely restrained in the rotational and vertical directions. Moreover, the inelastic one-degree-of-freedom system supported by the soil-pile system consists of a mass and a spring that transfers only the shear force between the footing and the superstructure. It is noted, therefore, that the results obtained here would be, to a certain extent, different from those obtained under realistic conditions. The equilibrium equation of the total system can be formulated as:

$$[M_T]\begin{Bmatrix}\ddot{u}_s\\ \ddot{u}_f\\ \ddot{u}_{21}\\ \ddot{u}_{22}\\ \ddot{u}_3\end{Bmatrix}+[C_T]\begin{Bmatrix}\dot{u}_s\\ \dot{u}_f\\ \dot{u}_{21}\\ \dot{u}_{22}\\ \dot{u}_3\end{Bmatrix}+[K_T]\begin{Bmatrix}u_s\\ u_f\\ u_{21}\\ u_{22}\\ u_3\end{Bmatrix}=\begin{Bmatrix}0\\0\\0\\0\\0\end{Bmatrix} \tag{29a}$$

where

$$[M_T]=\begin{bmatrix}[M_s] & [0]\\ [0] & [0]\end{bmatrix}+\begin{bmatrix}[0] & [0]\\ [0] & [M_N]_{N=2}\end{bmatrix} \tag{29b}$$

$$[C_T]=\begin{bmatrix}[C_s] & [0]\\ [0] & [0]\end{bmatrix}+\begin{bmatrix}[0] & [0]\\ [0] & [C_N]_{N=2}\end{bmatrix} \tag{29c}$$

$$[K_T]=\begin{bmatrix}[K_s] & [0]\\ [0] & [0]\end{bmatrix}+\begin{bmatrix}[0] & [0]\\ [0] & [K_N]_{N=2}\end{bmatrix} \tag{29d}$$

$$[M_s]=\begin{bmatrix}m_s & 0\\ 0 & m_f\end{bmatrix}$$

$$[C_s]=\begin{bmatrix} c_s & -c_s \\ -c_s & c_s \end{bmatrix}$$

$$[K_s]=\begin{bmatrix} k_s & -k_s \\ -k_s & k_s \end{bmatrix}$$

where u_s and u_f are the absolute displacements of the superstructure and the footing, respectively; u_{2i} and u_3 are the absolute displacements of the node in the *i* th core system and of the node at the right hand side of the Type II model, respectively; m_s and m_f are the masses of the superstructure and the footing, respectively; and c_s and k_s are the damping coefficient and the initial stiffness of the superstructure (pier), respectively. In order to estimate the response of the structural system, the absolute displacements are expressed by the sum of the displacements of the inertial response and the input motion, as follows:

$$\begin{Bmatrix} u_s \\ u_f \\ u_{21} \\ u_{22} \\ u_3 \end{Bmatrix} = \begin{Bmatrix} U_s \\ U_f \\ U_{21} \\ U_{22} \\ 0 \end{Bmatrix} + \begin{Bmatrix} 1 \\ 1 \\ 1 \\ 1 \\ 1 \end{Bmatrix} U_g \tag{30}$$

where U_g is the time-history input motion to the inertial system. Substituting Eq. 30 into Eq. 29 leads to

$$\begin{aligned} [\tilde{M}_T]\begin{Bmatrix} \ddot{U}_s \\ \ddot{U}_f \\ \ddot{U}_{21} \\ \ddot{U}_{22} \end{Bmatrix} + [\tilde{C}_T]\begin{Bmatrix} \dot{U}_s \\ \dot{U}_f \\ \dot{U}_{21} \\ \dot{U}_{22} \end{Bmatrix} + [\tilde{K}_T]\begin{Bmatrix} U_s \\ U_f \\ U_{21} \\ U_{22} \end{Bmatrix} &= -[M_g]\begin{Bmatrix} 1 \\ 1 \\ 1 \\ 1 \\ 1 \end{Bmatrix}\ddot{U}_g \\ &= -\begin{Bmatrix} m_s \\ m_f \\ 0 \\ 0 \end{Bmatrix}\ddot{U}_g \end{aligned} \tag{31}$$

where

$$\left[\tilde{M}_T\right]=\begin{bmatrix} m_s & 0 & 0 & 0 \\ 0 & m_f+\overline{M} & 0 & 0 \\ 0 & 0 & \overline{m}_1 & 0 \\ 0 & 0 & 0 & \overline{m}_2 \end{bmatrix},$$

$$\left[\tilde{C}_T\right]=\begin{bmatrix} c_s & -c_s & 0 & 0 \\ -c_s & c_s+C & 0 & 0 \\ 0 & 0 & c_1 & 0 \\ 0 & 0 & 0 & c_2 \end{bmatrix},$$

$$\left[\tilde{K}_T\right]=\begin{bmatrix} k_s & -k_s & 0 & 0 \\ -k_s & k_s+K+k_1+k_2 & -k_1 & -k_2 \\ 0 & -k_1 & k_1 & 0 \\ 0 & -k_2 & 0 & k_2 \end{bmatrix}, \text{ and}$$

$$\left[M_g\right]=\begin{bmatrix} m_s & 0 & 0 & 0 & 0 \\ 0 & m_f+\overline{M} & 0 & 0 & -\overline{M} \\ 0 & 0 & \overline{m}_1 & 0 & -\overline{m}_1 \\ 0 & 0 & 0 & \overline{m}_2 & -\overline{m}_2 \end{bmatrix}.$$

The inelasticity of the superstructure is assumed to be comparable to the Clough model (Clough and Johnson (1966)) that is generally used to model reinforced concrete members. The spring of the superstructure has a bi-linear skeleton curve where the ratio of the tangent stiffness to the initial stiffness is assumed to be $\alpha = 0.1$. The properties of the model are as follows: the masses of the superstructure and footing are $m_s = 500$ t and $m_f = 200$ t, respectively; the spring and dashpot coefficients of the superstructure (pier) are $k_s = 200000$ kN/m and $c_s = 400$ kN-sec/m, respectively; and the yielding displacement of the superstructure (pier) is 0.02 m. As an earthquake wave, Kobe NS (JMA) 1995 shown in Fig. 17 (a) is directly used as the input motion $\ddot{U}_g$ in Eq. 31, and the effects of input loss (e.g. Fan *et al.* (1991)) due to the existence of piles in the soil are not considered at all in this analysis. Time-history analysis is performed based on Eq. 31 by

using Newmark's β method ($\beta = 1/6$) as a numerical integration scheme, where the time interval Δt is 0.002 s. Moreover, the modified Newton-Raphson method is applied as a numerical iterative procedure for calculating the nonlinear response of the system. The above scheme and numerical method are well-known conventional techniques in time-history analysis of structural systems. In this analysis, an approximate solution calculated by using the Voigt model to represent the impedance function is also shown. The properties of the Voigt model are identical to the impedance function at $\omega \cong 0$ shown in Fig. 15, and are as follows: the spring coefficient is 240000 kN/m; and the damping coefficient is 21800 kN-sec/m.

The time-history response acceleration of the superstructure ($\ddot{u}_s$) can be estimated as shown in Fig. 17 (b). Fig. 17 (c) and (d) show that the displacement of the superstructure relative to the footing exceeds the elastic limit (0.02 m), and thus, an inelastic response appears in the analysis. This indicates that the frequency dependency of the impedance function can be quite easily considered in the nonlinear structural analysis by using the conventional numerical techniques. The results also show that a discrepancy appears in the responses when compared with the case of the Voigt model. This discrepancy occurs due to the frequency-dependent oscillations of the impedance function because the Type II model appropriately fits the impedance function, whereas the Voigt model is an approximate model that does not consider the frequency-dependent oscillations. In the analysis, it is expected that the inelastic response displacement of the pier in the case of the Type II model becomes larger than that in the case of the Voigt model. However, the amount of this discrepancy should carefully be considered since this example uses simplified conditions. At present, therefore, it is concluded that the effects of the frequency-dependent characteristics upon the response of inelastic structures may be quantitatively evaluated by using the present model with conventional numerical techniques.

CONCLUSIONS

In the present study, the following may be concluded:

1. A frequency-independent element called "gyro-mass" is proposed. The gyro-mass is defined as an independent unit system that generates a reaction force due to the relative acceleration of the nodes between which the gyro-mass is placed. A mechanical analogy is also presented for explaining the physical feasibility of the element. This element has the potential to generate various

types of impedance functions appearing in soil-structure interaction (SSI) problems. Moreover, a simple model that consists of the gyro-mass should (a) exhibit independence as a unit impedance system, and (b) describe the system in an identical manner to the actual treatment in the structural analysis.

2. Two types of simple models are proposed for simulating impedance functions that have cut-off frequencies and the impedance functions that have frequency-dependent oscillations. The model that simulates the former is called Type I, and the latter is called Type II. General formulae for these models are presented in the frequency domain. Moreover, matrix expressions that can be directly applied to conventional structural models are also presented. Rigorous impedance functions of single piles, soil reaction and pile groups are simulated by the model with good agreement. In addition, generalized models that contain multiple core systems are formulated to enhance the precision of the simulation results. The important feature of the present models is that the characteristics of the individual parameters are identified so that the fitting of impedance functions by using the models is fairly easy.

3. The proposed models can also simulate the rigorous impedance functions in the time domain. Moreover, this study demonstrates an example in which the Type II model is applied to the time-history analysis of a soil-pile-superstructure system with an inelastic structural member when subjected to an earthquake wave. Conventional numerical techniques can easily be applied to the time-history analysis. The present models and also various other types of models consisting of gyro-masses can be used to evaluate the effects of the frequency dependency of impedance functions upon nonlinear structural systems in advanced research.

NOTATION

The following symbols are used in this paper:

a	=	characteristic length of foundation;
a_0	=	dimensionless frequency;
α	=	ratio of tangent stiffness to initial stiffness;
β	=	coefficient appearing in Newmark's β method;
β_i	=	ratio of stiffness of *i*-th core system to base system;
β_s	=	material damping of soil;
c_s	=	shear wave velocity of soil;
d	=	diameter of pile;
D	=	damping ratio of soil;

E_p = Young's modulus of pile;

E_s = Young's modulus of soil;

γ_i = dimensionless coefficient of damper;

H = length of pile;

$i = \sqrt{-1}$ = imaginary unit;

I = geometrical moment of inertia of pile;

J = moment of inertia of disk;

$K_d^{(4)}$ = dynamic impedance of 4-pile group;

$K_s^{(1)}$ = static stiffness of single pile;

$\overline{m}$ = gyro-mass coefficient;

ν = Poisson's ratio of soil;

μ_i = dimensionless coefficient of gyro-mass;

r_0 = radius of pile;

$\overline{\rho}$ = ratio of mass density of soil to pile;

S = axis-to-axis distance of piles;

S_{w1} = real part of normalized impedance function of soil reaction in vertical direction;

S_{w2} = imaginary part of normalized impedance function of soil reaction in vertical direction;

ω = circular frequency;

Y = dimensionless parameter related to stiffness ratio of soil to pile.

REFERENCES

Baranov, V. A. (1967). "On the calculation of excited vibrations of an embedded foundation (*in Russian*)", *Voprosy Dynamiki I Prochnocti*, Polytechnical Institute of Riga, No. 14, 195-209.

Beredugo, Y. O., and Novak, M. (1972). "Coupled horizontal and rocking vibration of embedded footings", *Can. Geotech. J.*, 9 (4), 477-497.

Clough, R. W. and Johnson, S. B. (1966). "Effect of stiffness degradation on earthquake ductility requirements", *The second Earthquake Engrg. Sym., Proc.*, 227-232.

Dobry, R. and Gazetas, G. (1988). "Simple method for dynamic stiffness and damping of floating

pile groups", *Geotechnique*, 38, No. 4, 557-674.

Elsabee, F. and Morray, J. P. (1977). "Dynamic behavior of embedded foundations", *Research Report*, R77-33, Dep. of Civil Engrg., MIT. Cambridge, Mass.

Fan, K., Gazetas, G., Kaynia, A., Kausel, E., and Ahmad, S. (1991). "Kinematic seismic response of single piles and pile groups" *J. Geotech. Engrg.* ASCE, 117(12), 1860-1879.

Gazetas, G. (1991). "Formulas and charts for impedances of surface and embedded foundations" *J. Geotech. Engrg.* ASCE, 117(9), 1363-1381.

Kausel, E., and Roesset, J. M. (1975). "Dynamic Stiffness of Circular Foundations" *J. Engrg. Mech. Div.*, ASCE, Vol. 101, No. EM6, 770-1731.

Kaynia, A., and Kausel, E. (1982). "Dynamic stiffness and seismic response of pile groups" *Research Report*, R82-03, Dept. of Civil Engrg., MIT, Cambridge, Mass.

Makris, N. and Gazetas, G. (1993). "Displacement phase differences in a harmonically oscillating pile", *Geotechnique*, 43, No. 1, 135-150.

Meek, J. W. and Veletsos, A. S. (1974). "Simple models for foundations in lateral and rocking motion." *Proc*., 5*th World Conf. on Earthquake Engrg*., Vol. 2, Rome, Italy, 2610-2613.

Mylonakis, G. and Gazetas, G. (1998). "Vertical vibration and additional distress of grouped piles in layered soil" *Soils and Foundations*, JGS, Vol. 38, No.1, 1-14.

Nogami, T. and Novak, M. (1977). "Resistance of soil to a horizontally vibrating pile." *Earthquake Engrg. & Struct. Dyn.*, 5, 249-261.

Nogami, T. and Konagai, K. (1986). "Time domain axial response of dynamically loaded single piles." *J. Engrg. Mech.*, ASCE, 112(11), 1241-1252.

Nogami, T. and Konagai, K. (1988). "Time domain flexural response of dynamically loaded single piles." *J. Engrg. Mech.*, ASCE, 114(9), 1512-1525.

Novak, M. (1974). "Dynamic stiffness and damping of piles". *Can. Geotech. J.*, 11, 574-598.

Novak, M and Nogami, T. (1977). "Soil-pile interaction in horizontal vibration." *Earthquake Engrg. & Struct. Dyn.*, Vol. 5, 263-281.

Novak, M., Nogami, T., Konagai, K., and Aboul-Ella, F. (1978). "Dynamic soil reactions for plane strain case", *J. Engrg. Mech.*, ASCE, 104(4), 953-959.

Penzien, J., Scheffley, C. F., and Parmelee, F. A. (1964). "Seismic analysis of bridges on long piles" *J. Engrg. Mech. Div*., ASCE, EM3, 233-254.

Takemiya, H. and Yamada, Y. (1981). "Layered soil-pile-structure interaction." *Earthquake Engrg. & Struct. Dyn.*, 9, 437-452.

Veletsos, A. S. and Dotson, K. W. (1988). "Horizontal impedances for radially inhomogeneous viscoelastic soil layers", *Earthquake Engrg. & Struct. Dyn.*, 16, 947-966.

Journal of Engineering Mechanics, ASCE, Vol.133, No.10, pp.1101-1114, 2007. 10.

Wolf, J. P. and Somaini, D. R. (1986). "Approximate dynamic model of embedded foundation in time domain." *Earthquake Engrg. & Struct. Dyn.*, 14, 683-703.

Wolf, J. P. (1994). "Foundation vibration analysis using simple physical models." Eaglewood Cliffs, NJ: Prentice-Hall.

Wolf, J. P. and Song, C. (2002). "Some cornerstones of dynamic soil-structure interaction." *Engrg. Struct*., 24, 13-28.

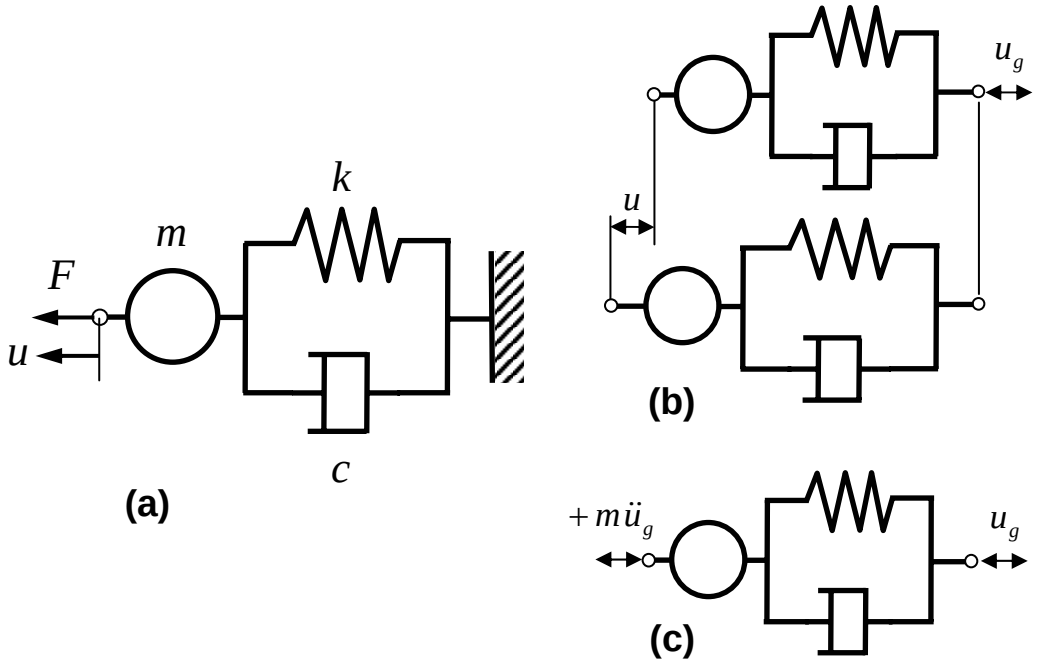

FIG.1 Spring-dashpot-mass system proposed by Penzien et al (1964)

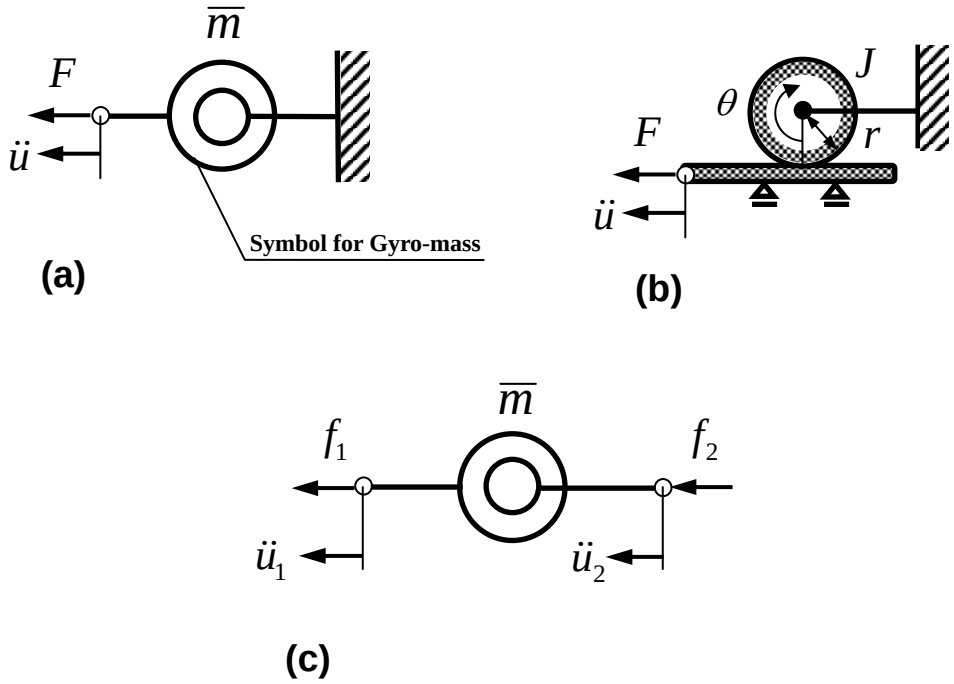

FIG. 2 Introduction of gyro-mass (a), mechanical analogy of gyro-mass (b), and relation between forces and displacements at nodes (c).

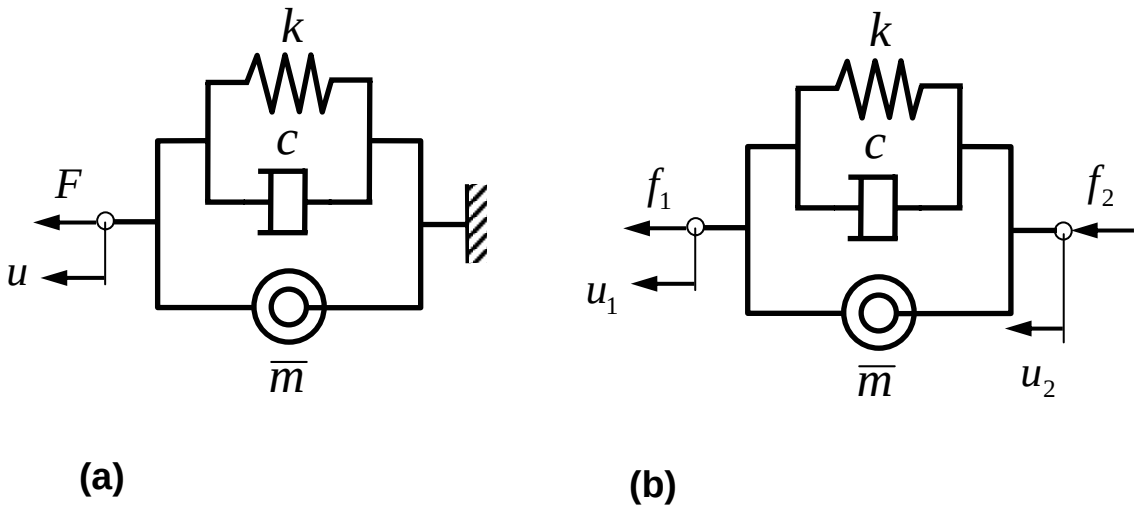

FIG. 3 Base system (a) and relation between forces and displacements at nodes (b).

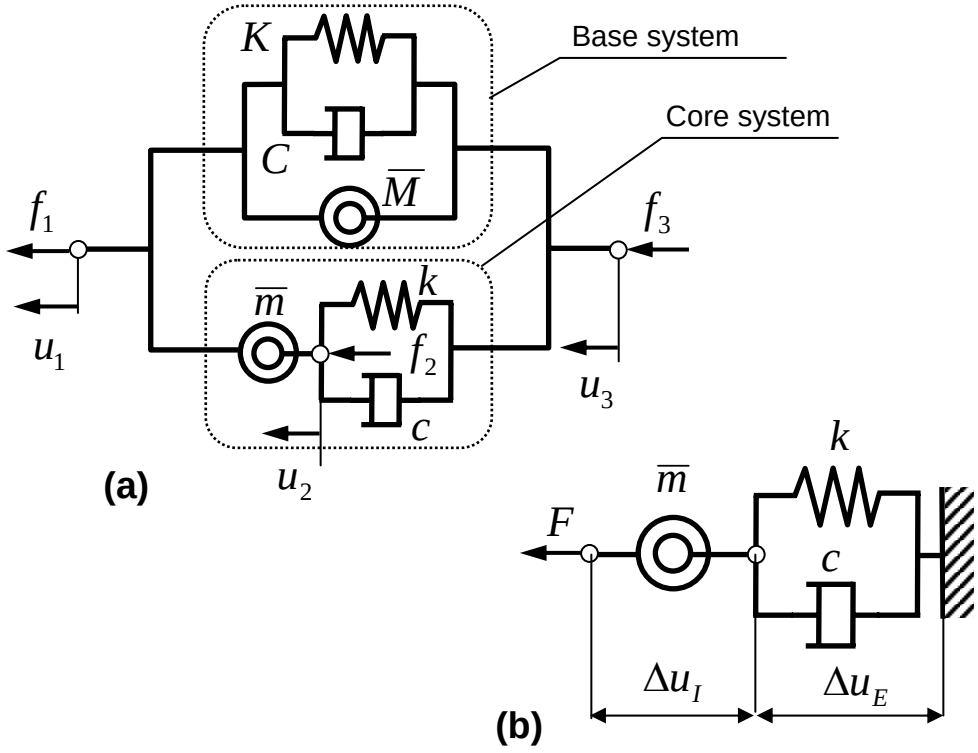

FIG. 4 Type I model (a) and its core system (b).

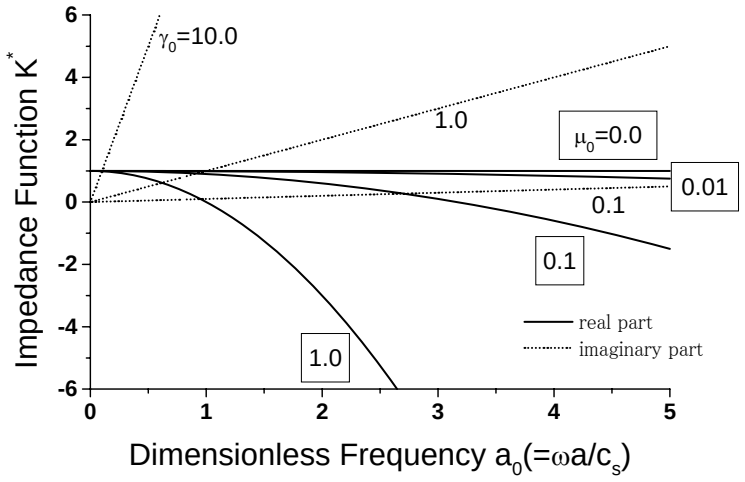

FIG. 5 Variation of impedance functions with coefficients μ_0 and γ_0 in base system ($K = 1.0$).

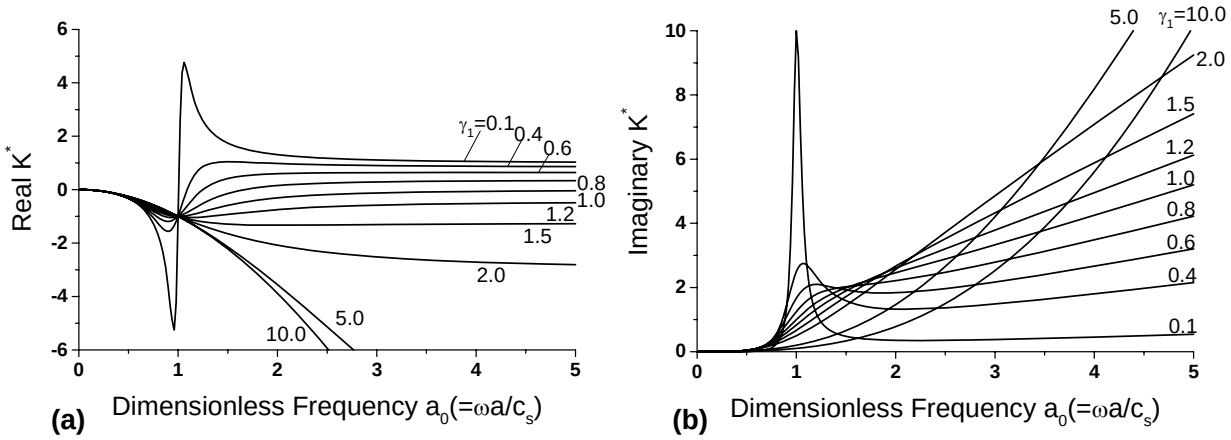

FIG. 6 Variation of impedance functions with several values of the coefficient γ_1 in core system of Type I model ($k = 1.0$ and $\mu_1 = 1.0$). (a) Real part (stiffness); (b) imaginary part (damping).

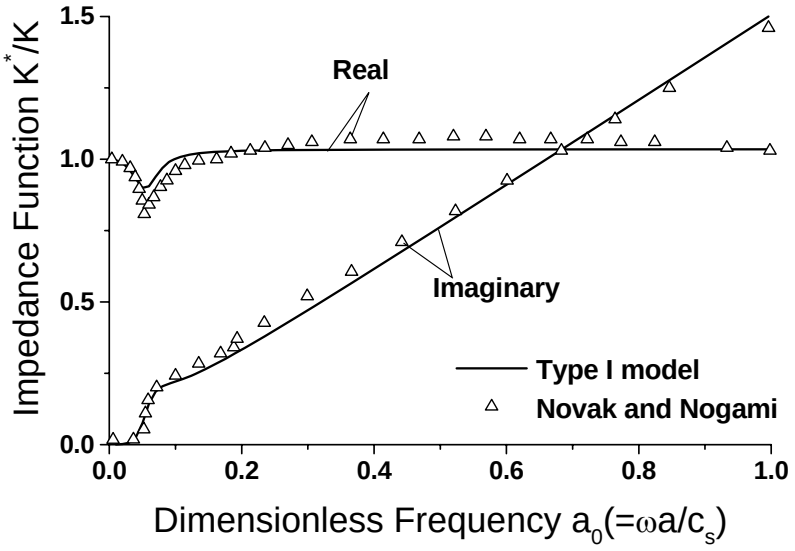

FIG. 7 Impedance functions of pile in vertical vibration simulated by using Type I model ($\gamma_0 = 0.1$, $\mu_0 = 0$, $\gamma_1 = 14$, $\mu_1 = 300$, $\beta_1 = 0.1$). Comparison with the rigorous solution of Novak and Nogami (1977).

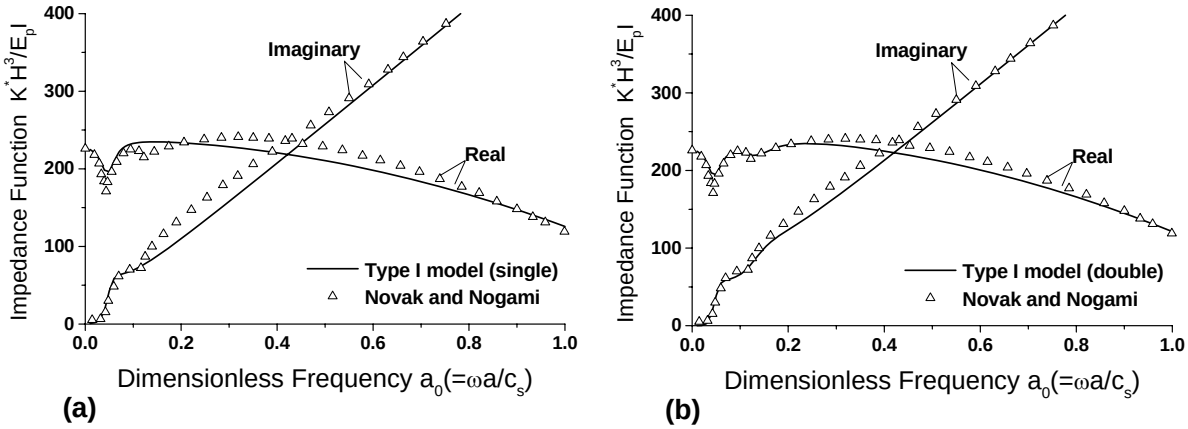

FIG. 8 Impedance functions of pile in horizontal vibration simulated by using Type I model. Comparison with the rigorous solution of Novak and Nogami (1977).

(a) $\gamma_0 = 0.3$, $\mu_0 = 0.5$, $\gamma_1 = 15$, $\mu_1 = 400$, $\beta_1 = 0.13$; **(b)** $\gamma_0 = 0$, $\mu_0 = 0.55$, $\gamma_1 = 15$, $\mu_1 = 400$, $\beta_1 = 0.13$, $\gamma_2 = 5$, $\mu_2 = 50$, $\beta_2 = 0.06$.

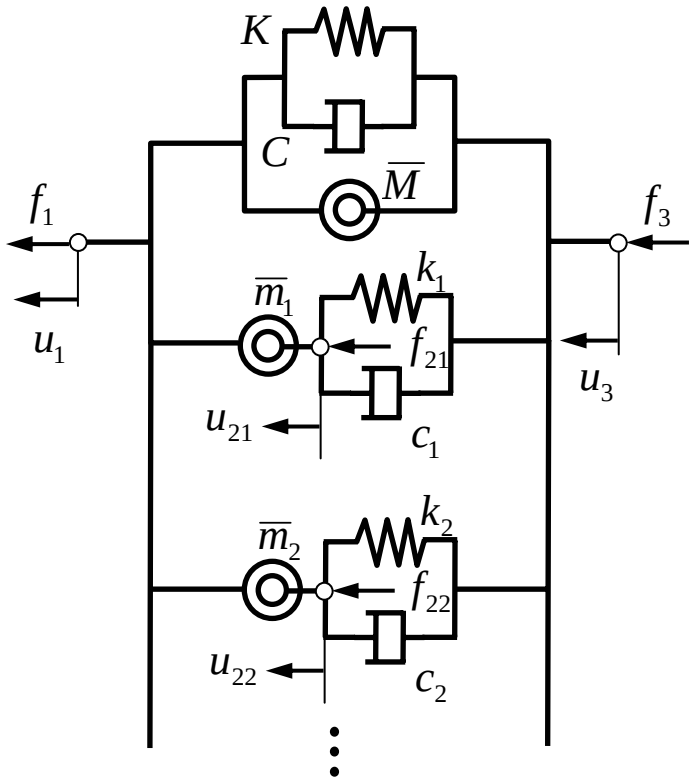

FIG. 9 Generalized Type I model.

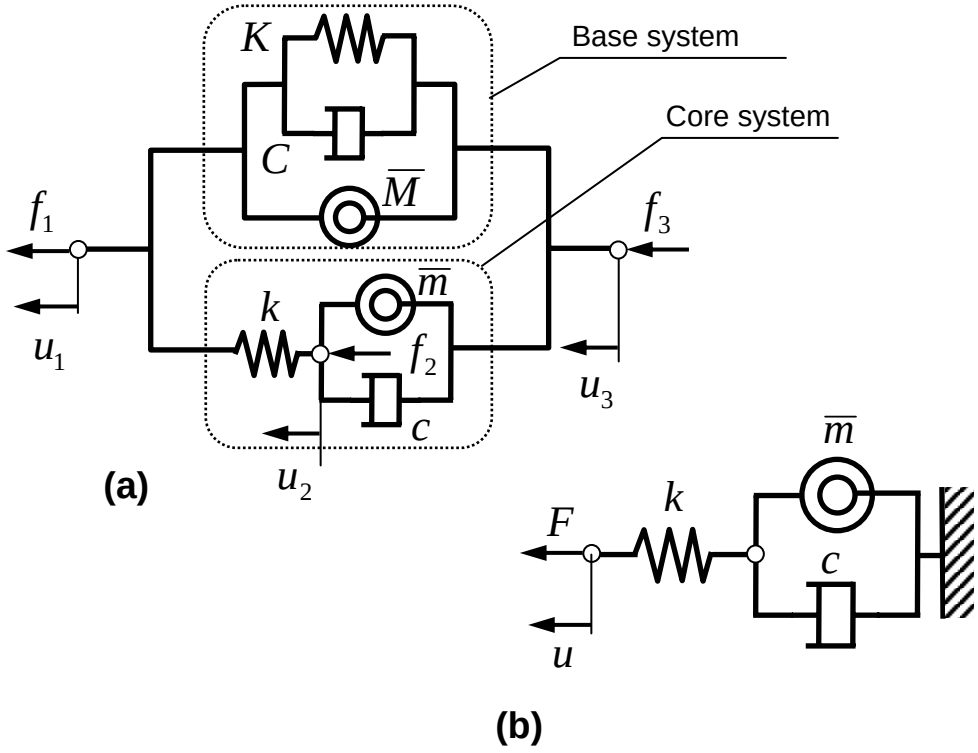

FIG.10 Type II model (a) and its core system (b)

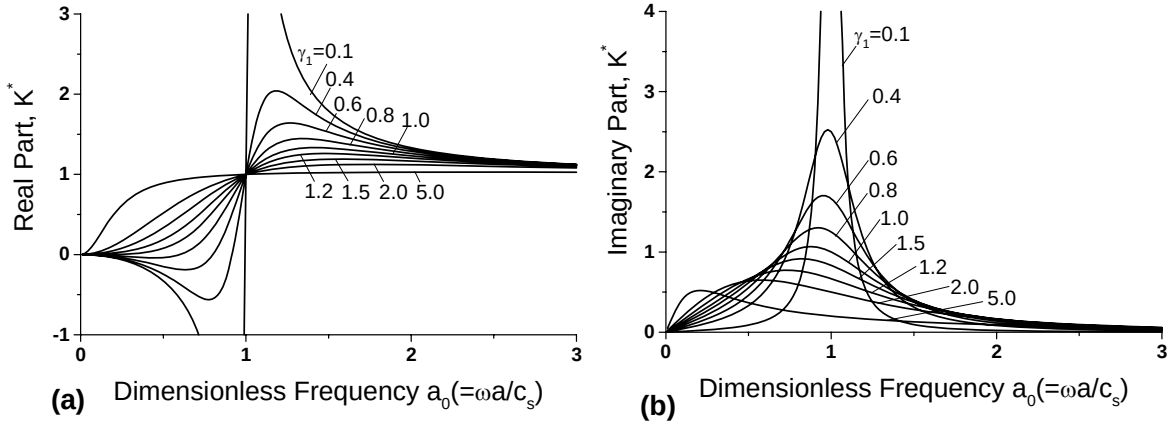

FIG. 11 Variation of impedance functions with several values of the coefficient γ_1 in core system of Type II model ($k = 1.0$ and $\mu_1 = 1.0$).
(a) Real part (stiffness); and (b) imaginary part (damping).

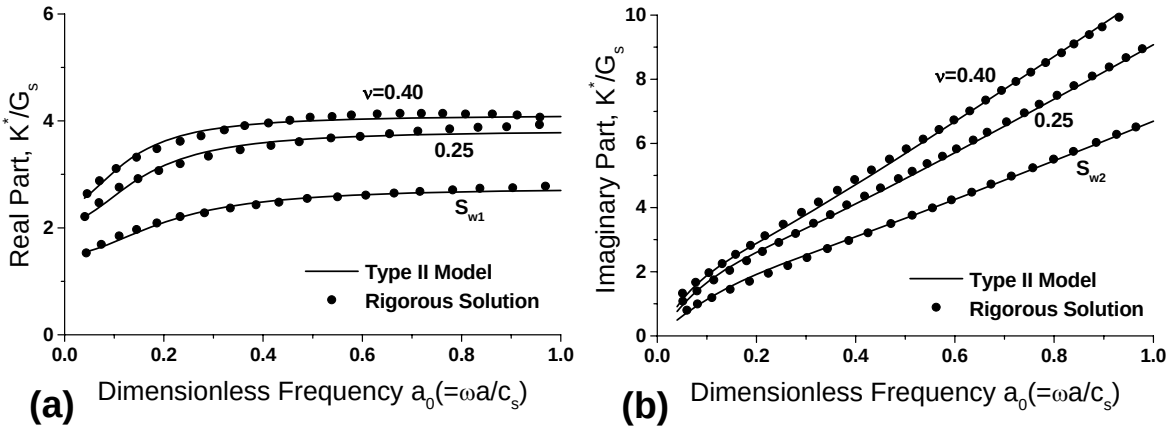

FIG. 12 Normalized impedance functions of soil reaction in horizontal vibration (Poisson's ratio ν =0.25 and 0.40) and in vertical vibration (real part S_{w1} and imaginary part S_{w2}) , showing (a) real part, and (b) imaginary part simulated by using Type II model. Comparison with the rigorous solution of Novak (1974) is also shown.

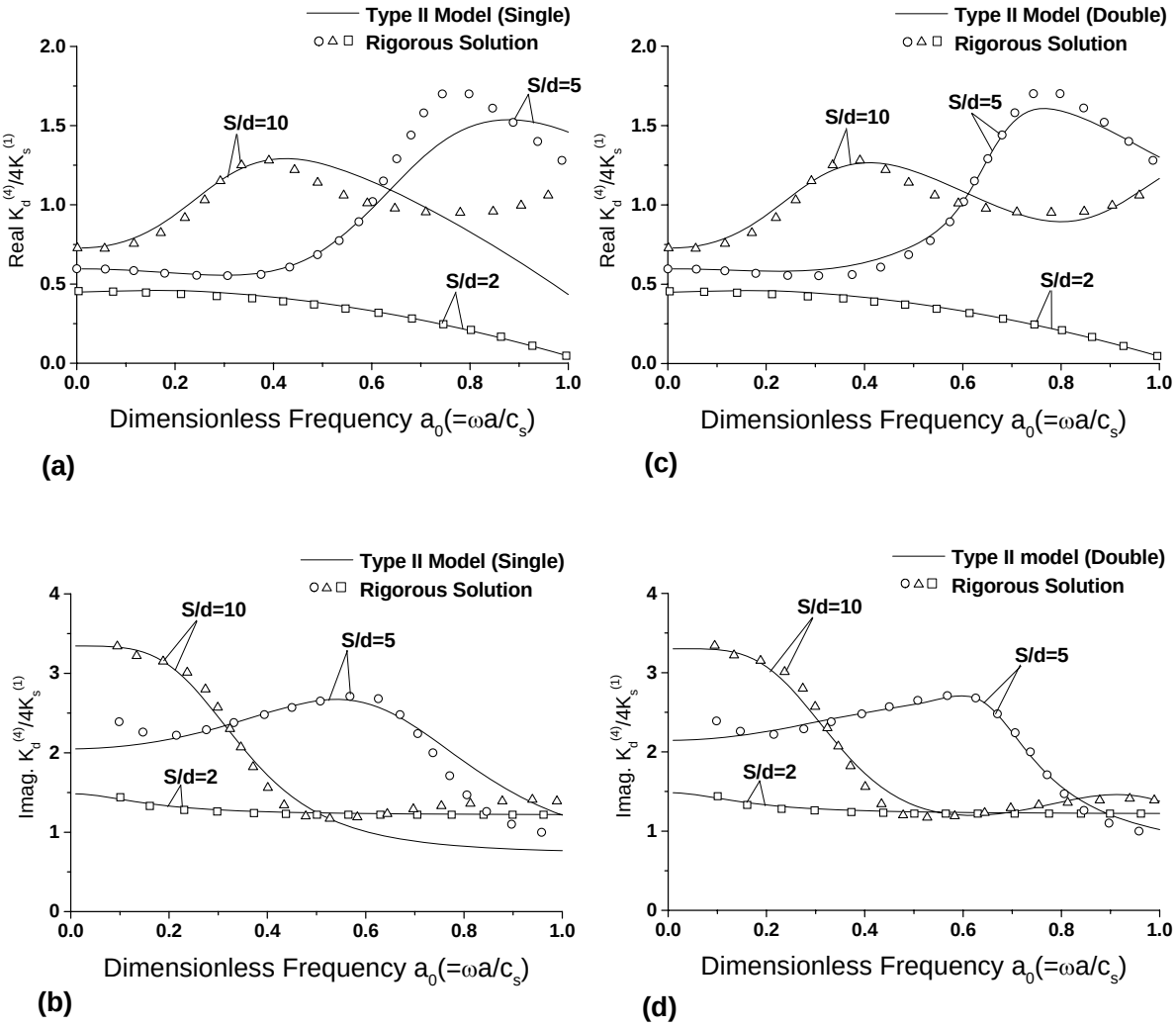

FIG. 13 Normalized horizontal impedance functions of a 2×2 pile group simulated by using Type II model ((a) and (b): single core system, (c) and (d): double core system). Comparison with the rigorous solution of Kaynia and Kausel (1982). (Imaginary part of the impedance is divided by the dimensionless frequency a_0; $K_d^{(4)}$ is the dynamic impedance of a 4-pile group; $K_s^{(1)}$ is the static stiffness of a single pile.)

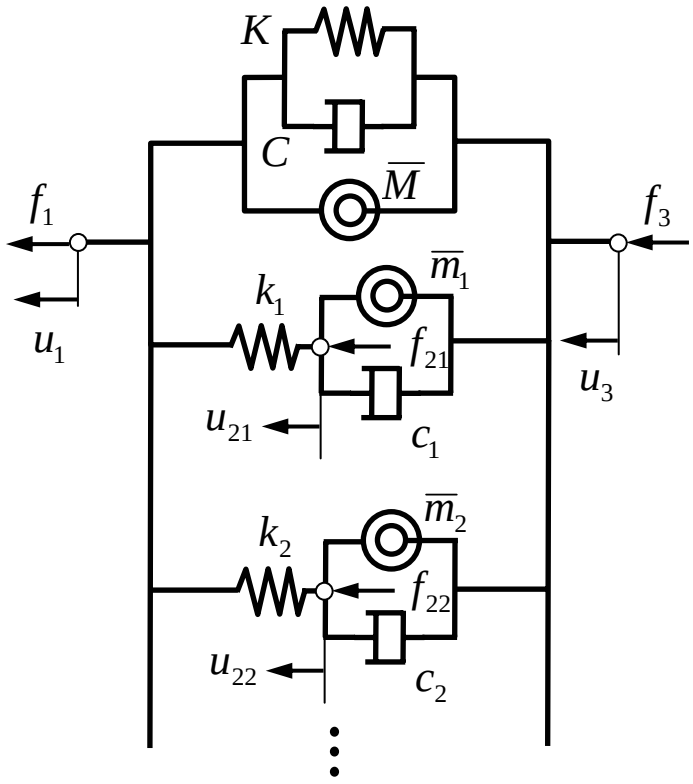

FIG. 14 Generalized Type II model.

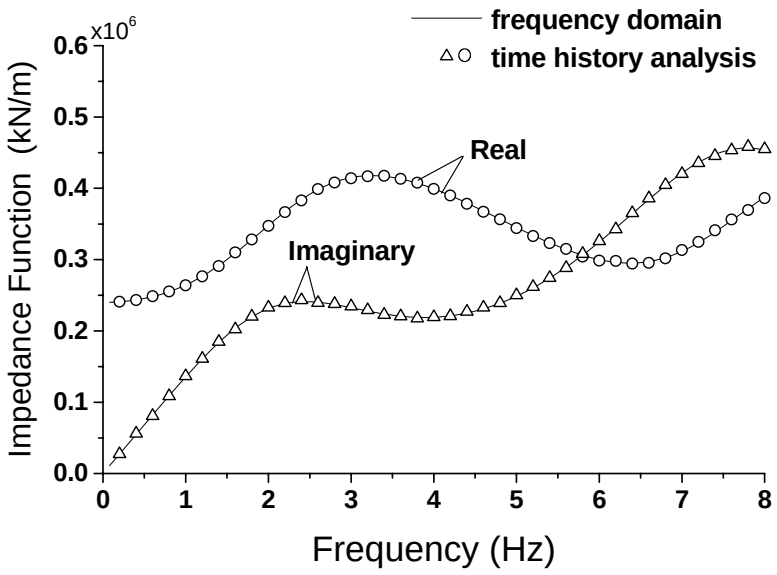

FIG. 15 Impedance functions of pile group in horizontal vibration ($S/d=10$) simulated by using Type II model in frequency domain compared with the numerical solution of time-history analysis.

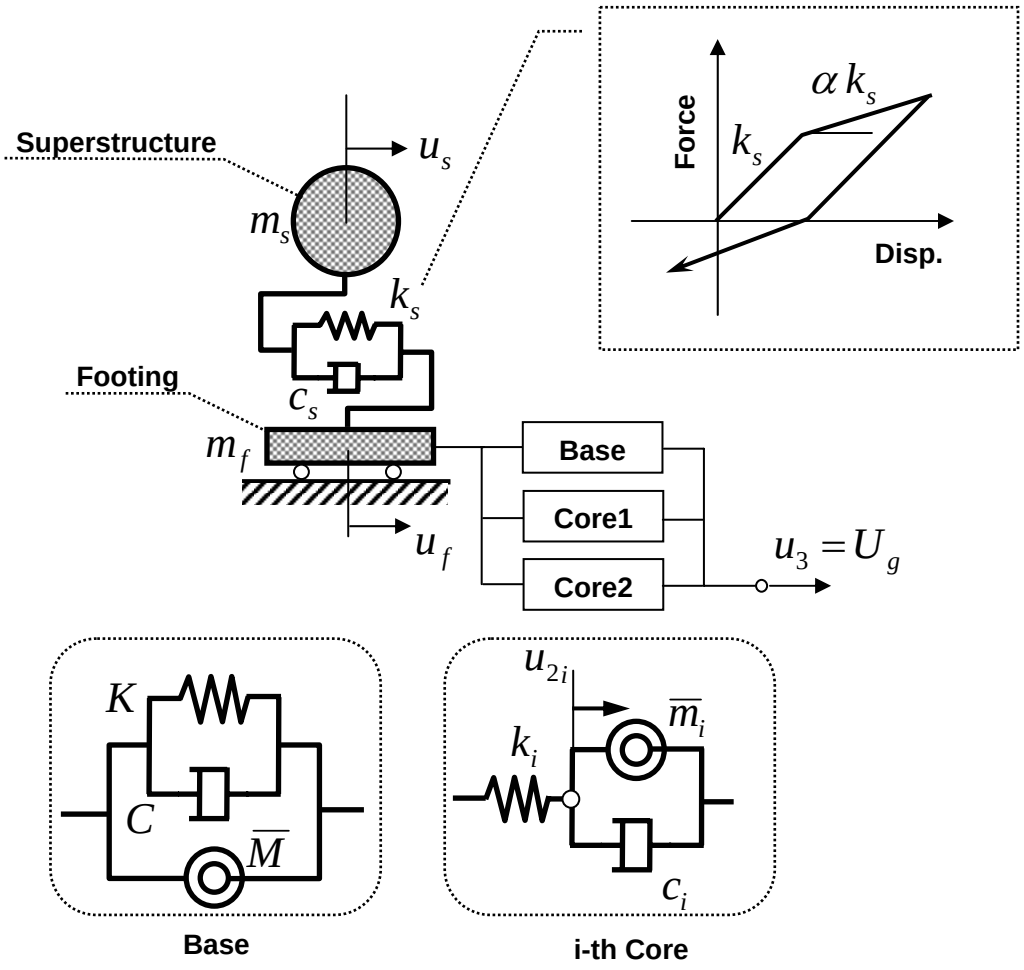

FIG. 16 Numerical model as application example of proposed model to nonlinear structural system.

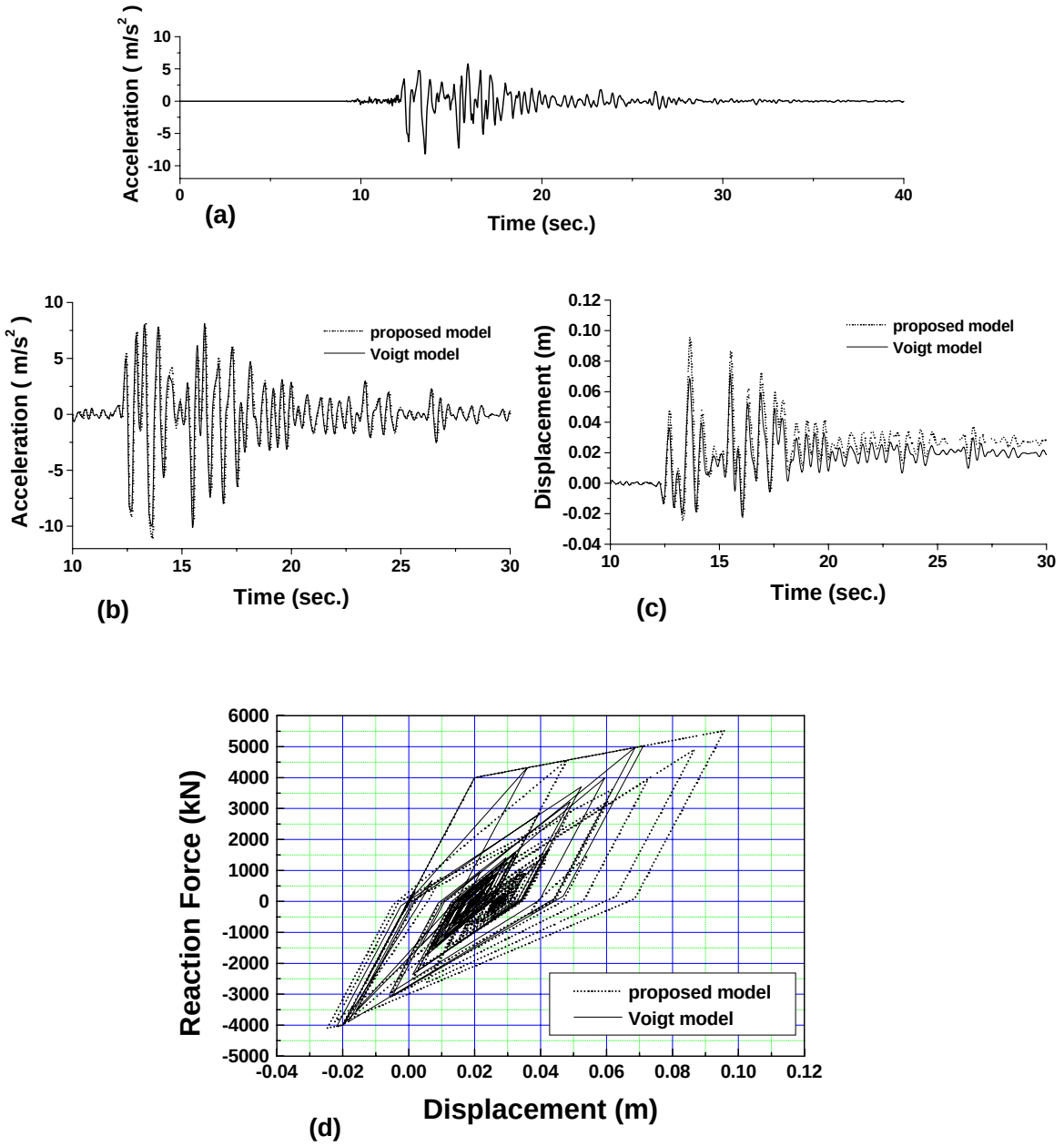

FIG. 17 Time-history responses of inelastic structural system. (a) Input motion (Kobe, JMA 1995); (b) Response acceleration of superstructure; (c) Relative displacement between superstructure and footing; (d) Hysteresis loop of superstructure (pier).

TABLE 1. Dimensionless coefficients of simple models simulating impedance functions of soil reaction

	Horizontal		Vertical
coefficient	$\nu = 0.25$	$\nu = 0.40$	S_{w1} and S_{w2}
K/G_s	2.10	2.40	1.50
γ_0	4.20	4.40	4.30
μ_0	0.00	0.00	0.00
β_1	0.80	0.70	0.80
γ_1	6.50	8.00	5.00
μ_1	1.00	1.00	1.00

TABLE 2. Dimensionless coefficients of simple models simulating impedance functions of a 2x2 pile group

	Single core systems			Double core systems		
coefficient	$S/d=2$	$S/d=5$	$S/d=10$	$S/d=2$	$S/d=5$	$S/d=10$
$K/4K_s^{(1)}$	0.45	0.60	0.73	0.45	0.60	0.73
γ_0	2.70	1.10	1.00	2.70	1.20	0.18
μ_0	1.00	1.00	1.40	1.00	1.00	1.30
β_1	0.10	1.80	0.90	0.10	0.40	0.94
γ_1	6.00	1.30	4.00	6.00	0.60	4.00
μ_1	1.00	1.90	8.00	1.00	2.30	8.00
β_2	-	-	-	0.00	1.20	1.00
γ_2	-	-	-	0.00	1.80	0.60
μ_2	-	-	-	0.00	2.50	0.95